

# Modification of Exchange Coupling in Fe/Nb/Fe/Pd Layered Structures using Hydrogen

M. WACHOWIAK<sup>a,\*</sup>, A. MARCZYŃSKA<sup>a</sup>, H. DAWCZAK-DEBICKI<sup>a,b</sup>,

M. PUGACZOWA-MICHALSKA<sup>a</sup>, S. PACANOWSKI<sup>a</sup>, Ł. MAJCHRZYCKI<sup>c</sup> AND L. SMARDZ<sup>a</sup>

<sup>a</sup>Institute of Molecular Physics, Polish Academy of Sciences, M. Smoluchowskiego 17, 60-179 Poznań, Poland

<sup>b</sup>Faculty of Physics, Adam Mickiewicz University, Umultowska 85, 61-614 Poznań, Poland

<sup>c</sup>WCZT, Adam Mickiewicz University, Umultowska 89C, 61-614 Poznań, Poland

Fe/Nb/Fe trilayers were prepared at room temperature using UHV magnetron sputtering. The interlayer exchange coupling energy was determined from a shift of the minor hysteresis loop from the origin. Results showed clear antiferromagnetic (AF) coupling maxima near  $\sim 6$  and 9 monolayers of Nb spacer. Calculations of the interlayer exchange coupling energy were carried out using *ab-initio* method with localized spin density approximations of exchange-correlation potential. The experimental results were in good agreement with *ab-initio* calculations. Furthermore, the position of the AF peaks and coupling energy values could be modified using hydrogen.

DOI: [10.12693/APhysPolA.133.609](https://doi.org/10.12693/APhysPolA.133.609)

PACS/topics: 75.70.-i, 68.55.-a

## 1. Introduction

In general, the magnetic properties of multilayers can be tailored by varying the composition, thickness and microstructure of the magnetic and non-magnetic sublayers. The strength and sign of the interlayer exchange coupling [1] could be tuned by alloying the spacer with nonmagnetic elements [2, 3] or using hydrogen [4, 5]. In the later case it could be changed not only by electronic structure but also thickness of the spacer. Furthermore, recently (001) oriented bcc-V/bcc-Fe multilayers were used as a model system of hydrogen absorbing thin film material to study the size effect [6]. Interlayer exchange coupling (IEC) across (110) textured niobium spacer in Nb/Fe multilayers was detected and characterized in Ref. [7, 8]. It was found that antiferromagnetic (AF) coupling oscillates with period of about 0.8-1 nm. However, the first AF peak was observed near 6 monolayers of Nb(110) spacer instead of expected by *ab-initio* calculations 2 monolayers [9]. The above behaviour was explained by a relatively big difference in the lattice parameter of Fe and Nb ( $\sim 13\%$ ).

Recently we have observed three AF peaks in the (110) oriented V/Fe multilayers [10] for  $1 \text{ nm} < d_V < 2.6 \text{ nm}$ . Results showed that the exchange coupling oscillates between a strong and weak AF coupling without transition to pure ferromagnetic (F) coupling [10]. Furthermore, we have reported in Ref. [11–12] that hydrogen could modify hysteresis loops and IEC of exchange coupled Fe/V/Fe trilayers.

In this paper we report on correlations between interlayer exchange coupling of the Fe sublayers and hydrogen

absorption of the niobium spacer in the Fe/Nb/Fe/Pd layered structures. According to Ref. [3] hydrogen can be absorbed exclusively in the Nb spacer. Therefore such studies could be potentially useful in hydrogen storage and sensors research as well as in the development of already existing various devices [13].

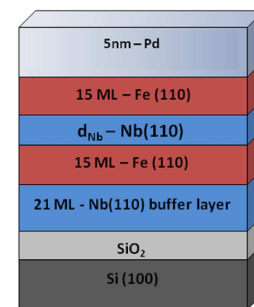


Fig. 1. Schematic description of prepared Fe/Nb/Fe trilayers.

## 2. Experimental procedure

Fe/Nb/Fe trilayers with constant-thickness Fe and step-like wedged (areas with constant-thickness) Nb sublayers were prepared at room temperature (RT) using ultra high vacuum (UHV) ( $5 \times 10^{-10}$  mbar) magnetron sputtering [14–16]. A protective layer of 5 nm Pd was used to allow a fast uptake and release of hydrogen [11, 12] at the room temperature and to avoid oxidation of the top Fe sublayers [17]. In Fig. 1 we show a schematic description of prepared Fe/Nb/Fe trilayers. As a substrate we have used Si(100) wafers with an oxidised surface to prevent a silicide formation. Therefore we have applied a special heat treatment in UHV

\*corresponding author; e-mail: [wachowiak@ifmpan.poznan.pl](mailto:wachowiak@ifmpan.poznan.pl)

before deposition in order to obtain an epitaxial SiO<sub>2</sub> surface layer [18]. The Fe-layers with a constant thickness of about 15 monolayers ( $\sim 3$  nm) were deposited using a direct current (DC) source. For preparation of the Nb-layers a radio frequency (RF) current source was used. The deposition rates of Nb and Fe were individually checked by quartz thickness monitors. The thickness of individual layers were controlled by varying their deposition times.

The chemical composition and the cleanness of all layers was checked *in-situ*, immediately after deposition, transferring the samples to an UHV ( $4 \times 10^{-11}$  mbar) analysis chamber equipped with X-ray photoelectron spectroscopy (XPS). Details of the XPS measurements can be found in Ref. [19–22].

The magnetic characterisation of the samples with constant-thickness sublayers was carried out using a Vibrating Sample Magnetometer (VSM) at RT. Before the measurements the step-like wedged Fe/Nb/Fe trilayer was cut in to pieces ( $4 \text{ mm} \times 15 \text{ mm}$ ) with constant thickness Fe and Nb sublayers. The exchange coupling fields were determined from a shift of the minor hysteresis loop [12]. Furthermore, the samples were hydrogenated at 1 bar pressure for 2 h at RT.

The calculations of the theoretical IEC and magnetic moment distribution in the Fe(15)/Nb( $d_{\text{Nb}}$ )/Fe(15) MLs with constant Fe (15 monolayers) and variable Nb sublayer thickness ( $d_{\text{Nb}}$ ) were also carried out. We have used the projector augmented wave (PAW) implementation of the Density Functional Theory (DFT) method of pseudopotentials (VASP code — Vienna *ab-initio* simulation package) [23–25]. The exchange-correlation energy was chosen in the local spin density approximation (LSDA) as well as in the generalized gradient approximation (GGA). The exchange-correlation functionals were based on the formulation of Perdew-Zunger (LSDA) [26] and Perdew-Burke-Ernzerhof (GGA) [27]. The calculations of the total energies of AF and F states of the system were performed for fully relaxed Fe/Nb( $d_{\text{Nb}}$ )/Fe layers stacked along the (110) direction with F and AF coupled magnetic slabs of Fe. The Hellmann–Feynman forces acting on the atoms have been used to perform a structural optimization of the systems. The planewave basis set used contained components with energies up to 400 eV. The presented results were obtained assuming the convergence threshold of  $10^{-6}$  eV in the total energies. The IEC was calculated in terms of the difference in total energy of the system in the two magnetic configurations F and AF coupled magnetic slabs:  $J(d_{\text{Nb}}) = E_{\text{F}}(d_{\text{Nb}}) - E_{\text{AF}}(d_{\text{Nb}})$ .

### 3. Results and discussion

In Fig. 2 we show XPS core level spectra of 2.5 nm – Fe, 5 nm – Nb, and 0.4 nm – Fe deposited on 5 nm – Nb underlayer. Practically no XPS signal was observed from potential contamination atoms like O:1s and C:1s.

AFM image of Fe/Nb/Fe trilayer with 5 monolayers of Nb spacer is shown in Fig. 3. The sample was covered by

a 5 nm Pd protective layer. Roughness parameters  $R_a$  and  $R_{\text{RMS}}$  measured on greater area ( $2 \mu\text{m} \times 2 \mu\text{m}$ ) were estimated as 0.21 nm and 0.26 nm, respectively. The relatively low value of the roughness parameters revealed planar growth of the layered sample in agreement with *in-situ* XPS studies of Nb growth on Fe underlayer, what is very similar to that reported recently for V/Fe bilayers [22].

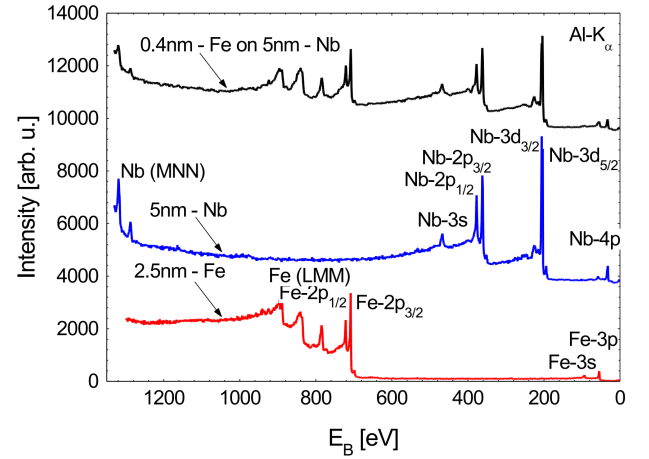


Fig. 2. XPS spectra (Al-K<sub>α</sub>) of pure 5 nm Nb, 2.5 nm Fe, and freshly deposited 0.4 nm Fe layer on 5nm Nb(110) underlayer.

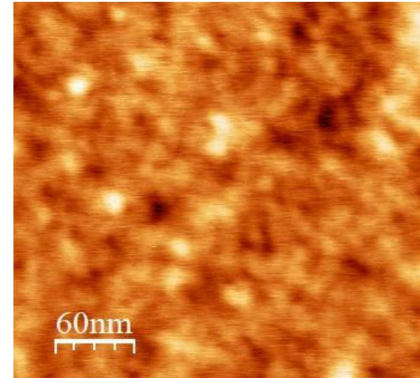


Fig. 3. AFM image of Fe(15)/Nb(5)/Fe(15) trilayer covered by a 5 nm Pd protective layer.

In Fig. 4 we show the theoretical distribution of the magnetic moments on Fe and Nb atoms in Fe/Nb/Fe trilayers with Nb spacer thickness equal to 6 monolayers. The magnetic moment on the Fe atoms is reduced compared to that measured for bulk material ( $2.2 \mu_{\text{B}}$ ), especially at the Fe-Nb and Nb-Fe interfaces. Furthermore, a small magnetic moment antiparallel to the Fe moment on the Nb atoms is induced near the interfaces (see Fig. 4).

Experimental results on IEC as a function of the Nb spacer thickness are shown in Fig. 5 (circles). Despite a relatively big difference in the lattice parameter of Fe

and Nb ( $\sim 13\%$ ). We have observed clear two local minima of IEC (maximum of AF coupling) located near  $d_{\text{Nb}} \sim 6$  and  $\sim 9$  monolayers. The results of theoretical calculations within LSDA (triangles in Fig. 5) also show two peaks of AF coupling for 6 and 8 monolayers of Nb spacer. The disagreement in the position of the experimental ( $\sim 9$  monolayers) and theoretical (8 monolayers) AF minima could be explained by alloying effect near Fe-Nb and Nb-Fe interfaces and different measurements (295 K) and calculation (0 K) temperature. Furthermore, the observed difference of the IEC presented in Fig. 5 and Ref. [7, 8] could be explained not only by different growth conditions but also by the different specific polarization of the niobium spacer near the Nb-Fe and Fe-Nb interfaces. Note, that after hydrogenation process (squares in Fig. 5) we have observed a transition from nearly zero to AF coupling for Nb spacer thickness of about 5 monolayers. Such a behavior reveals a possibility of modification of the IEC using hydrogen.

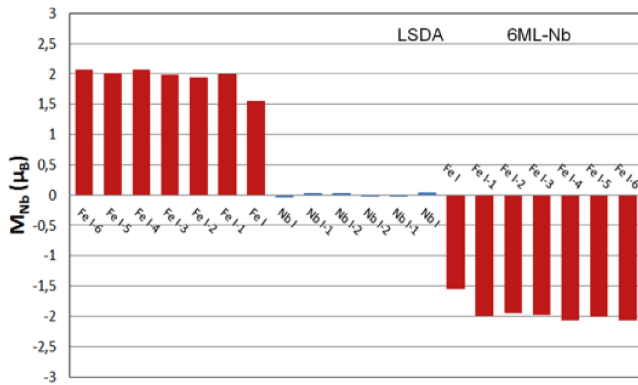


Fig. 4. Theoretical calculations of magnetic moment within LSDA for Fe(15)/Nb(6)/Fe(15) trilayers.

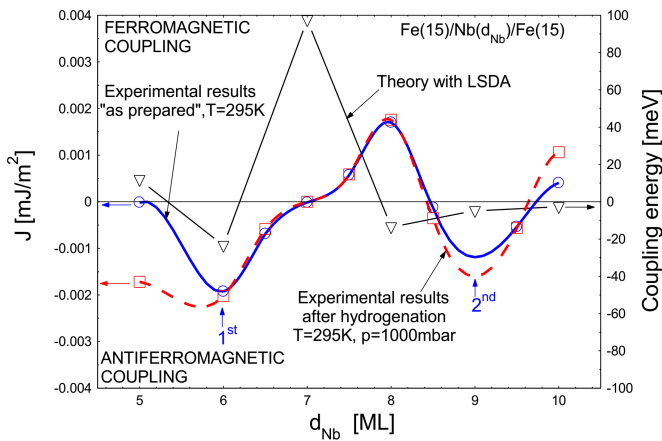


Fig. 5. Experimental results (circles) and theoretical calculations of the interlayer exchange coupling within LSDA (triangles) as a function of Nb(110) spacer thickness for Fe(15)/Nb( $d_{\text{Nb}}$ )/Fe(15) trilayers. Squares denote IEC after hydrogenation at RT.

In conclusion, we have found experimentally that the interlayer exchange coupling energy in the Fe/Nb/Fe trilayers strongly depends on the Nb spacer thicknesses and could be modified by hydrogen at room temperature. Antiferromagnetic coupling of the iron sublayers across niobium was also revealed by the *ab-initio* calculations.

## Acknowledgments

The first author (M.W.) would like to thank the Ministry of Science and Higher Education in Poland for financial support within the research project “Diamond grant”, 2017-21, No. DI2016011946.

## References

- [1] M. Ahlberg, E. Th Papaioannou, G. Nowak, B. Hjörvarsson, *J. Magn. Magn. Mater.* **341**, 142 (2013).
- [2] E. Holmström, A. Bergman, L. Nordström, I. A. Abrikosov, S. B. Dugdale, B.L. Györffy, *Phys. Rev. B* **70**, 064408 (2004).
- [3] B. Skubic, E. Holmström, D. Iusan, O. Bengone, O. Eriksson, R. Brucas, B. Hjörvarsson, V. Stancu, P. Nordblad, *Phys. Rev. Lett.* **96**, 057205 (2006).
- [4] F. Klöse, Ch. Rehm, D. Nagengast, H. Maletta, A. Weidinger, *Phys. Rev. Lett.* **78**, 1150 (1997).
- [5] B. Hjörvarsson, J.A. Dura, P. Isberg, T. Watanabe, T.J. Udovic, G. Andersson, C.F. Majkrzak, *Phys. Rev. Lett.* **79**, 901 (1997).
- [6] X. Xin, G. Pálsson, M. Wolff, B. Hjörvarsson, *Phys. Rev. Lett.* **113**, 046103 (2014).
- [7] Ch. Rehm, F. Klöse, D. Nagengast, H. Maletta, A. Weidinger, *Europhys. Lett.* **38**, 61 (1997).
- [8] J.E. Mattson, C.H. Sowers, A. Berger, S.D. Bader, *Phys. Rev. Lett.* **68**, 3252 (1992).
- [9] Nitya Nath Shukla, R. Prasad, *Phys. Rev. B* **70**, 014420 (2004).
- [10] A. Marczyńska, J. Skoryna, L. Smardz, *Acta Phys. Pol. A* **126**, 1315 (2014).
- [11] J. Skoryna, A. Marczyńska, M. Lewandowski, L. Smardz, *J. Alloys Comp.* **645**, 280 (2015).
- [12] J. Skoryna, M. Wachowiak, A. Marczyńska, A. Rogowska, Ł. Majchrzycki, W. Koczorowski, R. Czajka, L. Smardz, *Surf. Coat. Tech.* **303**, 119 (2016).
- [13] Wen-Chin Lin, Bo-Yao Wang, Han-Yuan Huang, Cheng-Jui Tsai, *J. All. Comp.* **661**, 20 (2016).
- [14] L. Smardz, *J. Alloys Comp.* **395**, 17 (2005).
- [15] L. Smardz, K. Smardz, H. Niedoba, *J. Magn. Magn. Mater.* **220**, 175 (2000).
- [16] L. Smardz, K. Le Dang, H. Niedoba, K. Chrzumnicka, *J. Magn. Magn. Mater.* **140-144**, 569 (1995).
- [17] H. Dawczak-Dębicki, A. Marczyńska, A. Rogowska, M. Wachowiak, M. Nowicki, S. Pacanowski, B. Jabłoński, R. Czajka, L. Smardz, *Acta Phys. Pol. A* **133**, 601 (2018).
- [18] See for example, *The Physics and Chemistry of SiO<sub>2</sub>, the Si-SiO<sub>2</sub> Interface*, Eds.: C.R. Helms, B.E. Deal, Plenum, New York 1988.

- [19] L. Smardz, M. Nowak, M. Jurczyk, *Int. J. Hydrogen Energy* **37**, 3659 (2012).
- [20] K. Smardz, L. Smardz, I. Okonska, M. Nowak, M. Jurczyk, *Int. J. Hydrogen Energy* **33**, 387 (2008).
- [21] L. Smardz, M. Jurczyk, M. Nowak, *Int. J. Hydrogen Energy* **37**, 3659 (2012).
- [22] A. Marczyńska, J. Skoryna, B. Szymański, L. Smardz, *Acta Phys. Pol. A* **127**, 552 (2015).
- [23] P.E. Blochl, *Phys. Rev. B* **50**, 17953 (1994).
- [24] G. Kresse, D. Joubert, *Phys. Rev. B* **59**, 1758 (1999).
- [25] G. Kresse, J. Furthmuller, *Phys. Rev. B* **54**, 11169 (1996).
- [26] J. P. Perdew, A. Zunger, *Phys. Rev. B* **23**, 5048 (1981).
- [27] J. P. Perdew, K. Burke, M. Ernzerhof, *Phys. Rev. Lett.* **77**, 3865 (1996).